J Mar Sci Technol (2017) 22:376–387
DOI 10.1007/s00773-016-0417-7

ORIGINAL ARTICLE

Observer-based adaptive output feedback tracking control of dynamically positioned surface vessels

Baris Bidikli[1,2] · Enver Tatlicioglu[1] · Erkan Zergeroglu[3]

Received: 6 January 2016 / Accepted: 11 October 2016 / Published online: 25 October 2016

Abstract In this work, we propose an observer-based adaptive output feedback tracking controller for dynamically positioned surface vessels. Specifically, to remove the velocity measurement dependency of the control formulation a nonlinear, model-free observer formulation have been proposed. The proposed observer does not make use of the system dynamics and together with the proposed controller structure ensure that the tracking error signal and the velocity estimation error asymptotically converges to zero. Stability of the closed-loop system is ensured by Lyapunov-based arguments. Simulation studies are also presented to illustrate the effectiveness of the proposed method.

Keywords Adaptive control · Observer-based control · Surface vessels

All the correspondence should be addressed to E. Tatlicioglu.

✉ Enver Tatlicioglu
enver@iyte.edu.tr

Baris Bidikli
baris.bidikli@deu.edu.tr

Erkan Zergeroglu
e.zerger@gtu.edu.tr

[1] Department of Electrical and Electronics Engineering, Izmir Institute of Technology, 35430 Izmir, Turkey

[2] Department of Mechatronics Engineering, Dokuz Eylul University, 35390 Izmir, Turkey

[3] Department of Computer Engineering, Gebze Technical University, 41400 Gebze, Kocaeli, Turkey

1 Introduction

Control of marine vehicles, especially slowly moving surface vessels, is extremely important in marine industry and is also an attractive research area because of the need for smooth operations and slow trajectory tracking. As a result, the development of automatic ship control systems has attracted the attention over the past decade. A fully actuated ship called as a dynamically positioned surface vessel has three degrees-of-freedom and it can be controlled via thrusters and propellers fore and aft of the ship [10, 14]. In earliest works, a simplified model, obtained by linearizing the system model about a set of pre-specified yaw angles [9], was used. This allowed linear control methods along with gain scheduling techniques to be utilized. PID controllers in cascade with a low-pass filter [2], linear optimal control laws in conjunction with Kalman filtering techniques [3, 11, 15] are examples of the linear controllers. To reduce the burden of control gain tuning process of PID-type controllers and extended Kalman filters, sliding mode control was evaluated to control vessel dynamic positioning systems in [1] and [17]. In [12], an H_∞ control design was developed for an approximate linear model of a ship dynamic positioning system. On the other hand, several control algorithms that take the nonlinear dynamically positioned surface vessels' dynamics into account have also been proposed to cope with the limitations of linearization [8, 19]. In [8], a class of nonlinear PD-type control laws for position regulation was developed; however, their robustness against parametric uncertainties cannot be guaranteed. To reduce the effects of parametric uncertainties and ensure robustness against unwanted environmental disturbances, higher order sliding mode controller was proposed in [16]. A robust nonlinear control law using singular perturbation theory that accounts

for parametric uncertainties and external disturbances was presented in [19]. Robust adaptive control approach with dynamic control allocation for the positioning of marine vessels equipped with a thruster-assisted mooring system, in the presence of parameter uncertainties, unknown disturbances, and nonlinearities, was presented in [6]. In [18], a model-reference adaptive control technique cascaded with adaptive Kalman filter was presented for dynamically positioned shuttle tanker. In our previous study [5], a novel continuous robust full-state feedback controller was designed for surface vessels that contains unstructured uncertainties in its system matrices.

Other past research has focused on designing control schemes that do not require velocity measurements. Motivated by this, in [9], Fossen and Grøvlen presented the design of a nonlinear output feedback controller using an observer backstepping method. Specifically, a nonlinear, model-based observer–controller couple was used to eliminate the need for velocity measurements while achieving global exponential position tracking. In [7], a velocity surrogate filter-based approach has been applied for adaptive output feedback control of surface vessels. The proposed method achieved global asymptotic tracking despite the lack of velocity measurements and uncertain system dynamics. In [20], Wondergem et al. proposed an observer-based output feedback tracking controller for fully actuated ships. The proposed controller achieved semi-global exponential stability provided the exact knowledge of the system parameters. Recently, in [4], we utilized an exact model knowledge observer–controller couple for tracking control of dynamically positioned surface vessels where only position and orientation measurements were available. A nonlinear model-free observer was designed to remove the velocity dependency of the control formulation.

The main aim of this work is the design of an output feedback tracking controller for dynamically positioned surface vessels. Our starting point for the proposed approach is the fact that the nonlinear ship model can be arranged in a form similar to the well-known, rigid-link, robot manipulator dynamic model. Using this fact, we propose a new model-free observer (i.e., the observer formulation does not make use of the system parameters) in conjunction with a desired ship model-based controller formulation. In assistance of the proposed observer, we can reconstruct the velocity information in contrast to [7] and other filter-based approaches. We would like to point out that there are some velocity measurement devices like gyro compass and global positioning systems (GPS), available for surface vessels. However, there exists some conditions where these devices may not work properly. To give an example, gyro compass does not work independently from the GPS and some external conditions like unexpected weather conditions might degradate the effectiveness of GPS. Therefore, obtaining a control structure independent of the velocity measurement might be considered as an important problem for surface vessels. Lyapunov-based stability analyses are utilized to demonstrate that the observer–controller couple ensures semi-global asymptotic position tracking for the nonlinear surface vessel dynamics despite parametric uncertainties using only position measurements.

The rest of the paper is organized in the following manner. Section 2 describes the mathematical model for the dynamically positioned ship along with its corresponding properties. The control objective and problem formulation are presented in Sect. 3, while the design and stability analysis are presented in Sect. 4. Numerical simulation results illustrating the performance of the proposed observer–controller scheme are given in Sect. 5. Section 6 contains concluding remarks.

2 System model and properties

The mathematical model for a dynamically positioned ship is represented by [10]

$$M\dot{v} + Dv = \tau \tag{1}$$

$$\dot{\eta} = R(\psi)v \tag{2}$$

where $\eta(t) \triangleq [x(t), y(t), \psi(t)]^T$ is the position of the ship containing translational positions in X- and Y- directions, and yaw angle, denoted by $x(t)$, $y(t)$ and $\psi(t)$, respectively, $v(t) \in \mathbb{R}^3$ represents the velocity of the ship, $\tau(t) \in \mathbb{R}^3$ represents the control input, $M \in \mathbb{R}^{3\times 3}$ is the uncertain constant, positive-definite, symmetric, mass inertia matrix, $D \in \mathbb{R}^{3\times 3}$ is the uncertain constant damping matrix, and $R(\psi) \in SO(3)$ is the rotation matrix between the earth and the body-fixed coordinate frames. The above mentioned system matrices have following structural forms

$$M = \begin{bmatrix} m_{11} & 0 & 0 \\ 0 & m_{22} & m_{23} \\ 0 & m_{23} & m_{33} \end{bmatrix}, \quad D = \begin{bmatrix} d_{11} & 0 & 0 \\ 0 & d_{22} & d_{23} \\ 0 & d_{32} & d_{33} \end{bmatrix}, \tag{3}$$

where their entries are constants, and the rotation matrix $R(\psi)$ has the form

$$R(\psi) = \begin{bmatrix} \cos(\psi) & -\sin(\psi) & 0 \\ \sin(\psi) & \cos(\psi) & 0 \\ 0 & 0 & 1 \end{bmatrix}. \tag{4}$$

After substituting (2) and its time derivative into (1), a compact representation of the mathematical model can be obtained as

$$J\ddot{\eta} + C\dot{\eta} + F\dot{\eta} = \tau^* \tag{5}$$

where dynamic terms $J(\eta)$, $C(\eta,\dot{\eta})$, $F(\eta) \in \mathbb{R}^{3\times 3}$ (see Appendix A), and the control input, $\tau^*(t) \in \mathbb{R}^3$ are defined as

$$J \triangleq RMR^T, \quad C \triangleq RM\dot{R}^T, \quad F \triangleq RDR^T, \quad \tau^* \triangleq R\tau \tag{6}$$

where the orthogonality of the rotation matrix (*i.e.*, $R^{-1} = R^T$) was utilized.

The dynamic model given by (5) satisfies following properties.

Property 1 *The inertia matrix $J(\eta)$ is symmetric, positive-definite, and satisfies the following bounds*

$$m_l I_3 \le J \le m_u I_3 \tag{7}$$

$$\frac{1}{m_u} I_3 \le J^{-1} \le \frac{1}{m_l} I_3 \tag{8}$$

where m_l, $m_u \in \mathbb{R}$ are positive bounding constants, and $I_3 \in \mathbb{R}^{3\times 3}$ is the standard identity matrix defined as

$$I_3 \triangleq \begin{bmatrix} 1 & 0 & 0 \\ 0 & 1 & 0 \\ 0 & 0 & 1 \end{bmatrix}. \tag{9}$$

Property 2 *The dynamic terms $J(\eta)$ and $C(\eta,\dot{\eta})$ satisfy the skew–symmetric relationship*

$$\varphi^T \left(\frac{1}{2}\dot{J} - C \right) \varphi = 0 \; \forall \varphi \in \mathbb{R}^3. \tag{10}$$

Property 3 *The dynamic term $C(\eta,\dot{\eta})$ satisfies the relationship*

$$C(\varphi,\phi)\kappa = C(\varphi,\kappa)\phi \quad \forall \varphi,\phi,\kappa \in \mathbb{R}^3. \tag{11}$$

Property 4 *The dynamic terms $J(\cdot)$, $C(\cdot)$, $F(\cdot)$ satisfy the following bounds*

$$\|J(\varphi) - J(\phi)\|_{i\infty} \le \zeta_{j1}\|\varphi - \phi\| \tag{12}$$

$$\left\|J^{-1}(\varphi) - J^{-1}(\phi)\right\|_{i\infty} \le \zeta_{j2}\|\varphi - \phi\| \tag{13}$$

$$\|C(\varphi,\phi)\|_{i\infty} \le \zeta_{c1}\|\phi\| \tag{14}$$

$$\|C(\varphi,\phi) - C(\kappa,\phi)\|_{i\infty} \le \zeta_{c2}\|\phi\|\|\varphi - \kappa\| \tag{15}$$

$$\|F(\varphi)\|_{i\infty} \le \zeta_{f1} \tag{16}$$

$$\|F(\varphi) - F(\phi)\|_{i\infty} \le \zeta_{f2}\|\varphi - \phi\| \tag{17}$$

$\forall \varphi,\ \phi,\ \kappa \in \mathbb{R}^3$, ζ_{j1}, ζ_{j2}, ζ_{c1}, ζ_{c2}, ζ_{f1}, $\zeta_{f2} \in \mathbb{R}$ are positive bounding constants, and $\|\cdot\|_{i\infty}$ denotes the induced infinity norm.

Property 5 *The mathematical model of the ship given in (5) can be linearly parameterized as*

$$Y(\eta,\dot{\eta},\ddot{\eta})\theta \triangleq J(\eta)\ddot{\eta} + C(\eta,\dot{\eta})\dot{\eta} + F(\eta)\dot{\eta}, \tag{18}$$

where $Y(\eta,\dot{\eta},\ddot{\eta}) \in \mathbb{R}^{3\times 9}$ denotes the regression matrix and $\theta \in \mathbb{R}^9$ is a constant vector containing system parameters and defined as

$$\theta \triangleq [m_{11} \quad m_{22} \quad m_{23} \quad m_{33} \quad d_{11} \quad d_{22} \quad d_{23} \quad d_{32} \quad d_{33}]^T \tag{19}$$

with its entries being defined in Appendix A.

The linearly parameterized form of the mathematical model of the ship given in (18) can be written in terms of the desired position and its time derivatives as

$$Y_d(\eta_d,\dot{\eta}_d,\ddot{\eta}_d)\theta \triangleq J(\eta_d)\ddot{\eta}_d + C(\eta_d,\dot{\eta}_d)\dot{\eta}_d + F(\eta_d)\dot{\eta}_d \tag{20}$$

where $Y_d(\eta_d,\dot{\eta}_d,\ddot{\eta}_d) \in \mathbb{R}^{3\times 9}$ is a function of the desired position and its first and second time derivatives, denoted by $\eta_d(t)$, $\dot{\eta}_d(t)$, $\ddot{\eta}_d(t) \in \mathbb{R}^3$, respectively.

3 Problem formulation

Our objective is to design a position tracking controller for the dynamically positioned ship when only the position of the ship $\eta(t)$ is measurable and the velocity of the ship is unavailable. The control problem is further complicated by the parametric uncertainty, that is, the constant parameter vector θ introduced in (18) being uncertain.

To quantify the tracking objective, the position tracking error, denoted by $e(t) \in \mathbb{R}^3$, is defined as

$$e \triangleq \eta_d - \eta. \tag{21}$$

In the subsequent analysis, the desired position and its first three time derivatives are assumed to be bounded.

To compensate for the lack of velocity measurements, a velocity observer, denoted by $\hat{\dot{\eta}}(t) \in \mathbb{R}^3$, will be designed subsequently. To facilitate the velocity observer design, a velocity observation error, denoted by $\tilde{\dot{\eta}}(t) \in \mathbb{R}^3$, and the corresponding position observation error, denoted by $\tilde{\eta}(t) \in \mathbb{R}^3$, are defined as

$$\tilde{\dot{\eta}} \triangleq \dot{\eta} - \hat{\dot{\eta}} \tag{22}$$

$$\tilde{\eta} \triangleq \eta - \hat{\eta} \tag{23}$$

where $\hat{\eta}(t) \in \mathbb{R}^3$ is the observed position. To facilitate the subsequent stability analysis and to simplify the error system development, two filtered errors are defined as follows

$$r \triangleq \dot{e} + \alpha e \tag{24}$$

$$s \triangleq \tilde{\dot{\eta}} + \alpha\tilde{\eta} \tag{25}$$

where $r(t) \in \mathbb{R}^3$ is the filtered position tracking error, $s(t) \in \mathbb{R}^3$ is the filtered velocity observation error, and $\alpha \in \mathbb{R}$ is a positive constant control gain.

4 Control design

In this section, the observer–controller couple is designed for the dynamically positioned ship. The subsequent development is based on the restrictive assumption that the position and orientation of the ship is the only state that is available for control design.

4.1 Observer–controller couple design

Based on the subsequent stability analysis, the velocity observer is designed as

$$\dot{\hat{\eta}} = p + K_0\tilde{\eta} - K_c e, \tag{26}$$

where $p(t) \in \mathbb{R}^3$ is an auxiliary filter signal updated according to

$$\dot{p} = K_1 \mathrm{Sgn}(\tilde{\eta}) + \mathrm{K_2}\tilde{\eta} - \alpha \mathrm{K_c e}, \tag{27}$$

where K_0, K_c, K_1, $K_2 \in \mathbb{R}^{3\times3}$ are diagonal, positive-definite gain matrices, and $\mathrm{Sgn}(\cdot) \in \mathbb{R}^3$ is the vector signum function.

The subsequent stability analysis enabled us to design the control input $\tau^*(t)$ in the following form

$$\tau^* = Y_d\hat{\theta} + K_p e + \alpha K_c(\eta_d - \hat{\eta}) + K_c(\dot{\eta}_d - \dot{\hat{\eta}}) \tag{28}$$

where $K_p \in \mathbb{R}^{3\times3}$ is a diagonal, positive-definite control gain matrix and the parameter estimate vector $\hat{\theta}(t) \in \mathbb{R}^9$ is generated according to the following update rule

$$\dot{\hat{\theta}} = \mathrm{Proj}\left\{\Gamma\left(\mathrm{Y_d^T e} - \int_0^t \frac{\mathrm{d}}{\mathrm{d}\sigma}\{\mathrm{Y_d^T}(\sigma)\}\mathrm{e}(\sigma)\mathrm{d}\sigma + \alpha\int_0^t \mathrm{Y_d^T}(\sigma)\mathrm{e}(\sigma)\mathrm{d}\sigma\right)\right\}, \tag{29}$$

where $\Gamma \in \mathbb{R}^{9\times9}$ is a constant, diagonal, positive-definite, adaptation gain matrix and $\mathrm{Proj}\{\cdot\} \in \mathbb{R}^9$ is a projection operator. It should be noted that, the subsequent stability analysis requires the boundedness of $\hat{\theta}(t)$ and its time derivative. The projection algorithm in (29) is introduced to guarantee the boundedness of $\hat{\theta}(t)$ and $\dot{\hat{\theta}}(t)$. The projection operator satisfies the following property (which will later be utilized in the stability analysis)

$$\tilde{\theta}^T\Gamma^{-1}\mathrm{Proj}\{\Gamma Y_d^T r\} \le \tilde{\theta}^T Y_d^T r \tag{30}$$

where $\tilde{\theta}(t) \in \mathbb{R}^9$ is the parameter estimation error defined as

$$\tilde{\theta} \triangleq \theta - \hat{\theta}. \tag{31}$$

After utilizing (21) and (23), the following expression may be obtained

$$\eta_d - \hat{\eta} = e + \tilde{\eta}. \tag{32}$$

The above formulation and its time derivative can be utilized along with (28) to rewrite the control input in the following advantageous form

$$\tau^* = Y_d\hat{\theta} + K_p e + K_c(r + s). \tag{33}$$

4.2 Observer analysis

In this section, a preliminary Lyapunov-like analysis will be performed for the observer error dynamics. Specifically, after utilizing (5), time derivative of (26) and (27) along with the time derivative of (22), we obtain velocity observation error dynamics as

$$\ddot{\tilde{\eta}} = \ddot{\eta} - \ddot{\hat{\eta}} \tag{34}$$

$$= N_0 - K_1\mathrm{Sgn}(\tilde{\eta}) - K_2\tilde{\eta} - K_0\dot{\tilde{\eta}} + K_c r, \tag{35}$$

where $N_0(t) \in \mathbb{R}^3$ is an auxiliary term defined as

$$N_0 \triangleq J^{-1}(\tau^* - C\dot{\eta} - F\dot{\eta}). \tag{36}$$

After substituting (20) and (33) into (36), the auxiliary term $N_0(t)$ can be partitioned as

$$N_0 = N_d + N_b, \tag{37}$$

where $N_d(t)$, $N_b(t) \in \mathbb{R}^3$ are auxiliary terms defined as

$$N_d \triangleq -\left|J^{-1}(\eta_d)\right|Y_d\tilde{\theta} + \left|J^{-1}(\eta_d)\right|J(\eta_d)\ddot{\eta}_d \tag{38}$$

$$\begin{aligned} N_b \triangleq\ & \left[J^{-1}(\eta_d) - J^{-1}(\eta)\right]Y_d\tilde{\theta} + J^{-1}(\eta)\left[K_p e + K_c(r+s)\right] \\ & + \left[J^{-1}(\eta) - J^{-1}(\eta_d)\right]J(\eta_d)\ddot{\eta}_d + J^{-1}(\eta)[C(\eta_d,\dot{\eta}_d)\dot{\eta}_d \\ & - C(\eta,\dot{\eta})\dot{\eta} + F(\eta_d)\dot{\eta}_d - F(\eta)\dot{\eta}]. \end{aligned} \tag{39}$$

Remark 1 After exploiting the boundedness properties of desired trajectory and the projection algorithm, we can show that both $N_d(t)$ and its time derivative are bounded. Furthermore, based on its definition in (39), the norm of $N_b(t)$ can be upper bounded as

$$\|N_b\| \le \rho_{01}\|e\| + \rho_{02}\|r\| + \rho_{03}\|e\|\|r\| + \rho_{04}\|r\|^2 + \rho_{05}\|s\|, \tag{40}$$

where ρ_{01}, ρ_{02}, ρ_{03}, ρ_{04}, $\rho_{05} \in \mathbb{R}$ are known positive bounding constants (see Sect. 8 for details).

We can obtain the following dynamics for the filtered observation error $s(t)$

$$\dot{s} = N_d + N_b - K_1\mathrm{Sgn}(\tilde{\eta}) - K_2\tilde{\eta} - K_0\dot{\tilde{\eta}} + K_c r + \alpha\dot{\tilde{\eta}}, \tag{41}$$

where (35) and (37) were utilized. After selecting the observer gains α, K_0 and K_2 to satisfy

$$\alpha(K_0 - \alpha I_3) = K_2 \tag{42}$$

the expression in (41) can be rearranged as

$$\dot{s} = N_d + N_b - K_1 \mathrm{Sgn}(\widetilde{\eta}) - \frac{\mathrm{K}_2}{\alpha}\mathrm{s} + \mathrm{K}_c\mathrm{r}, \tag{43}$$

where (25) was utilized.

The form of the filtered observation error dynamics in (43) enables us to state the following preliminary Lyapunov-like analysis. We define the following non-negative scalar function, denoted by $V_0(t) \in \mathbb{R}$,

$$V_0 \triangleq \frac{1}{2}s^T s + P, \tag{44}$$

where $P(t) \in \mathbb{R}$ is an auxiliary non-negative function defined as

$$P \triangleq \zeta_P - \int_0^t \omega(\sigma)d\sigma, \tag{45}$$

where $\omega(t)$, $\zeta_P \in \mathbb{R}$ are defined as

$$\omega \triangleq s^T(N_d - K_1 \mathrm{Sgn}(\widetilde{\eta})) \tag{46}$$

$$\zeta_P \triangleq \sum_{i=1}^{3} K_{1i}|\widetilde{\eta}_i(0)| - \widetilde{\eta}^T(0)N_d(0). \tag{47}$$

As presented in (9), if the entries of K_1 are chosen to satisfy

$$K_{1i} \geq |N_{di}(t)| + \frac{1}{\alpha}\left|\dot{N}_{di}(t)\right| \forall t \in \mathbb{R}, \quad i = 1, 2, 3, \tag{48}$$

where $K_{1i} \in \mathbb{R}$ denotes the ith diagonal entry of K_1, and $N_{di}(t)$, $\dot{N}_{di}(t)$ denote the ith entries of $N_d(t)$, $\dot{N}_d(t)$, respectively, then $P(t)$ is non-negative. Hence, $V_0(t)$ is a valid Lyapunov function. The time derivative of $V_0(t)$ can be obtained as

$$\dot{V}_0 = s^T\left(-\frac{1}{\alpha}K_2 s + N_b + K_c r\right), \tag{49}$$

where (43) and the time derivative of (45) were utilized.

4.3 Error system development

To obtain the dynamics for the filtered tracking error $r(t)$, we pre-multiply its time derivative with J, then utilize (5) and (21), and after performing some straightforward algebraic manipulations, we reach

$$J\dot{r} = -Cr + Y_s\theta - \tau^*, \tag{50}$$

where $Y_s(t) \in \mathbb{R}^{3\times 9}$ is a regressor matrix and $Y_s(t)\theta$ is defined as

$$Y_s\theta = J(\ddot{\eta}_d + \alpha\dot{e}) + C(\dot{\eta}_d + \alpha e) + F\dot{\eta}. \tag{51}$$

After substituting the control input in (33) into (50), we can reach the following closed-loop error dynamics for $r(t)$

$$J\dot{r} = -Cr + \chi - K_p e - K_c(r + s) + Y_d\tilde{\theta}, \tag{52}$$

where $\chi(t) \in \mathbb{R}^3$ is an auxiliary error-like term defined as

$$\chi \triangleq Y_s\theta - Y_d\theta. \tag{53}$$

Remark 2 Based on its definition in (53), the norm of the auxiliary term $\chi(t)$ can be upper bounded as

$$\|\chi\| \leq \rho_1(\|e\|)\|e\| + \rho_2(\|e\|)\|r\|, \tag{54}$$

where $\rho_1(\|e\|)$, $\rho_2(\|e\|) \in \mathbb{R}$ are known positive non-decreasing functions of their arguments (see (8) for details).

4.4 Stability analysis

In this section, the stability of the closed-loop system is investigated.

Theorem 1 *The velocity observer in* (26) *and* (27), *the control input of* (28), *and the adaptation law in* (29) *ensure semi-global asymptotic stability of the closed-loop system in the sense that*

$$\|e(t)\|, \left\|\dot{\tilde{\eta}}(t)\right\| \to 0 \quad \text{as} \quad t \to +\infty \tag{55}$$

provided that $\alpha K_{p,\min} \geq 1$, *controller and observer gains are selected to satisfy* (42) and (48), *and the controller gain* K_c *and the observer gain* K_2 *are chosen as*

$$K_c = \left(1 + \rho_2 + k_n\rho_1^2\right)I_3, \tag{56}$$

$$K_2 = \alpha\left(1 + \rho_{05} + k_n\left(\rho_{01}^2 + \rho_{02}^2 + \rho_{03}^2 + \rho_{04}^2\right)\right)I_3, \tag{57}$$

where $\rho_1(\|e\|)$, $\rho_2(\|e\|)$ *were introduced in* (54), ρ_{0i}, $i = 1, \ldots, 5$ *were introduced in* (40), *and* $k_n \in \mathbb{R}$ *is a nonlinear damping gain selected to satisfy the following condition*

$$k_n > \frac{1}{2} + \frac{\lambda_2}{2\lambda_1}\|z(0)\|^2 \tag{58}$$

and $z(t) \in \mathbb{R}^{19}$ *is defined as*

$$z \triangleq \left[\sqrt{P} \quad s^T \quad r^T \quad e^T \quad \tilde{\theta}^T\right]^T \tag{59}$$

and the positive bounding constants λ_1, $\lambda_2 \in \mathbb{R}$ *are defined as*

$$\lambda_1 \triangleq \frac{1}{2}\min\left\{1, J_{\min}, K_{p,\min}, \frac{1}{\lambda_{\min}(\Gamma)}\right\} \tag{60}$$

$$\lambda_2 \triangleq \max\left\{1, \frac{J_{\max}}{2}, \frac{K_{p,\max}}{2}, \frac{1}{2\lambda_{\max}(\Gamma)}\right\} \tag{61}$$

where subscripts min *and* max *denote the minimum and maximum eigenvalues of a matrix, respectively.*

Proof A non-negative Lyapunov function, denoted by $V(z) \in \mathbb{R}$, is defined as

$$V \triangleq V_0 + \frac{1}{2} r^T J r + \frac{1}{2} e^T K_p e + \frac{1}{2} \tilde{\theta}^T \Gamma^{-1} \tilde{\theta}. \tag{62}$$

The above Lyapunov function can be upper and lower bounded as

$$\lambda_1 \|x\|^2 \leq \lambda_1 \|z\|^2 \leq V \leq \lambda_2 \|z\|^2, \tag{63}$$

where $x(t) \in \mathbb{R}^9$ is defined as

$$x \triangleq \begin{bmatrix} s^T & r^T & e^T \end{bmatrix}^T. \tag{64}$$

The time derivative of $V(t)$ is obtained as

$$\dot{V} = \dot{V}_0 + r^T J \dot{r} + \frac{1}{2} r^T \dot{J} r + e^T K_p \dot{e} - \tilde{\theta}^T \Gamma^{-1} \dot{\hat{\theta}} \tag{65}$$

and after utilizing (10), (24), (29), time derivative of (29), (49), (52), we obtain

$$\dot{V} \leq s^T N_b - \frac{1}{\alpha} s^T K_2 s + r^T \chi - r^T K_c r - \alpha e^T K_p e. \tag{66}$$

After applying the upper bounds in (40) and (54), the right-hand side of (66) can be upper bounded as

$$\begin{aligned} \dot{V} \leq & -\alpha K_{p,\min} \|e\|^2 - \|r\|^2 - \|s\|^2 \\ & + \left[\rho_{01} \|e\| \|s\| - k_n \rho_{01}^2 \|s\|^2 \right] \\ & + \left[\rho_{02} \|r\| \|s\| - k_n \rho_{02}^2 \|s\|^2 \right] \\ & + \left[\rho_{03} \|e\| \|r\| \|s\| - k_n \rho_{03}^2 \|s\|^2 \right] \\ & + \left[\rho_{04} \|r\|^2 \|s\| - k_n \rho_{04}^2 \|s\|^2 \right] \\ & + \left[\rho_1 \|e\| \|r\| - k_n \rho_1^2 \|r\|^2 \right], \end{aligned} \tag{67}$$

where (56) and (57) were utilized. After completing the squares of the bracketed terms, the right-hand side of (67) can be upper bounded as

$$\begin{aligned} \dot{V} \leq & -\left[\alpha K_{p,\min} - \frac{1}{2k_n} - \frac{1}{2k_n} \|r\|^2 \right] \|e\|^2 \\ & - \left[1 - \frac{1}{4k_n} - \frac{1}{4k_n} \|r\|^2 \right] \|r\|^2 - \|s\|^2. \end{aligned} \tag{68}$$

After utilizing (64) the right-hand side of (68) can be obtained in a more compact form as

$$\dot{V} \leq -\left[1 - \frac{1}{2k_n} (1 + \|x\|^2) \right] \|x\|^2. \tag{69}$$

The sign of the upper bound of $\dot{V}(t)$ is determined by the bracketed term in (69), and this term has to be non-negative to ensure the negative semi-definiteness of $\dot{V}(t)$, that is, to ensure the negative semi-definiteness of $\dot{V}(t)$, we must have

$$1 - \frac{1}{2k_n} (1 + \|x\|^2) > 0. \tag{70}$$

After utilizing (63), a sufficient condition on (70) can be obtained as follows

$$1 - \frac{1}{2k_n} \left(1 + \frac{V}{\lambda_1} \right) > 0 \tag{71}$$

and hence the right-hand side of (69) can be reformulated as

$$\dot{V} \leq -\beta \|x\|^2 \text{ provided that } 2k_n > 1 + \frac{V}{\lambda_1} \tag{72}$$

where $\beta \in \mathbb{R}$ is some positive constant satisfying $0 < \beta \leq 1$. Due to the negative semi-definiteness of $\dot{V}(t)$, the maximum value that $V(t)$ can have is its initial value $V(0)$, therefore, after utilizing (63), a more conservative condition on k_n can be obtained to have the following form

$$\dot{V} \leq -\beta \|x\|^2 \text{ provided that } 2k_n > 1 + \frac{\lambda_2}{\lambda_1} \|z(0)\|^2, \tag{73}$$

that is, when k_n is selected to satisfy (58), we can ensure that $V(t)$ is bounded. Given the boundedness of $V(t)$, it is clear that $z(t) \in \mathcal{L}_\infty$, and thus, $e(t)$, $r(t)$, $s(t)$, $P(t)$, $\tilde{\theta}(t) \in \mathcal{L}_\infty$. After utilizing standard signal chasing arguments, we can show that all signals in the closed-loop system are bounded, and $e(t)$ and $\dot{\tilde{\eta}}(t)$ are uniformly continuous signals (from the boundedness of their time derivatives). Furthermore, after integrating both sides of (73), we can conclude that $x(t) \in \mathcal{L}_2$, and therefore $e(t)$, $\dot{\tilde{\eta}}(t) \in \mathcal{L}_2$. Finally, after utilizing Barbalat's Lemma [13], the asymptotic tracking result given in (55) can be obtained. □

5 Numerical simulation results

To illustrate the performance of the observer–controller couple, a numerical simulation with Matlab Simulink was performed. The ship model in (1) was utilized with the following mass inertia and damping matrices [9]

$$M = \begin{bmatrix} 1.0852 & 0 & 0 \\ 0 & 2.0575 & -0.4087 \\ 0 & -0.4087 & 0.2153 \end{bmatrix}, \tag{74}$$

$$D = \begin{bmatrix} 0.08656 & 0 & 0 \\ 0 & 0.0762 & 0.1510 \\ 0 & 0.0151 & 0.0031 \end{bmatrix}. \tag{75}$$

The desired position of the ship was given as

$$\eta_d = [\,10\sin(0.2t) \quad 10\cos(0.2t) \quad 5\sin(0.2t)\,]^T \tag{76}$$

with the initial positions $\eta(0) = [\,1[m] \quad -1[m] \quad 1[\text{deg}]\,]^T$, and the initial velocities $\dot{\eta}(0)$ were set to zero. To illustrate the performance of the controller in a more realistic scenario, we have included sensor noise into the system, an additive zero mean Gaussian noise with 40 dB signal-to-noise ratio was applied to position measurements. To examine the results in a comparative manner, simulations were performed for both the proposed observer-based adaptive controller and an conventional proportional integral derivative (PID) type controller.

For the proposed observer-based adaptive controller, the controller and observer gains were tuned via a trial-and-error method until a good tracking performance was achieved, and were chosen as

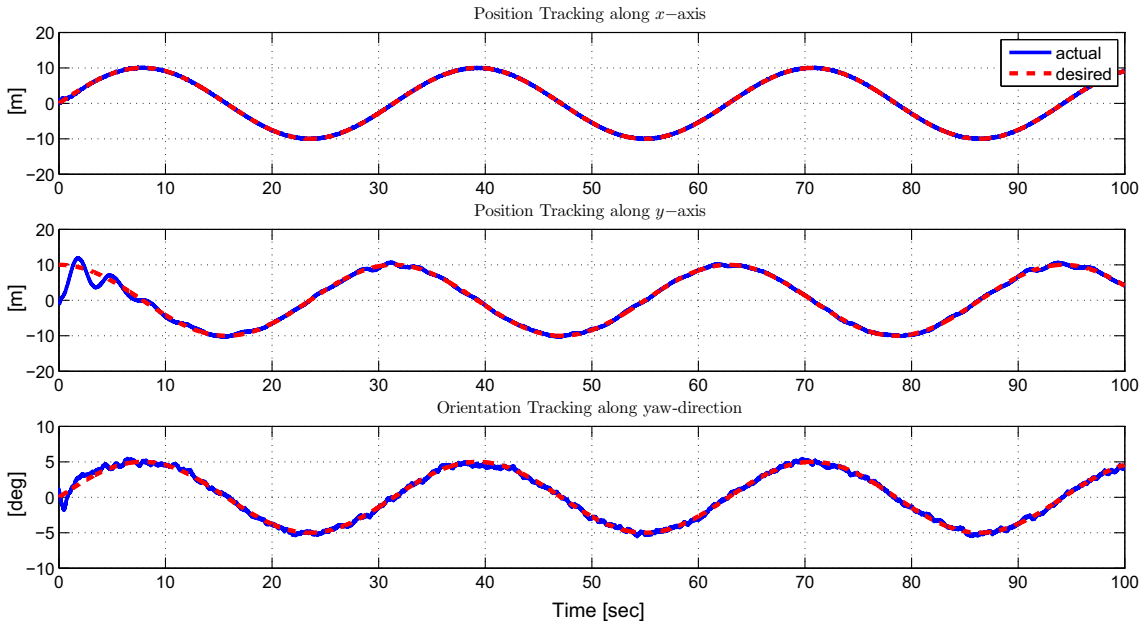

Fig. 1 The desired position $\eta_d(t)$ (*dotted*) and the actual position $\eta(t)$ (*solid*) for adaptive controler

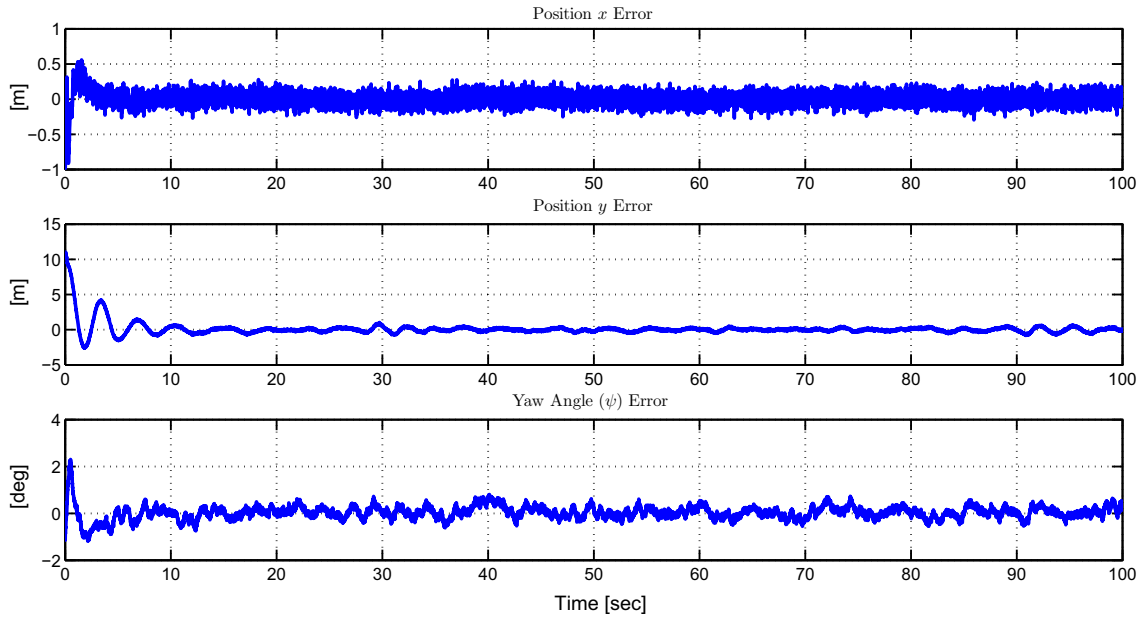

Fig. 2 The tracking error $e(t)$ for adaptive controller

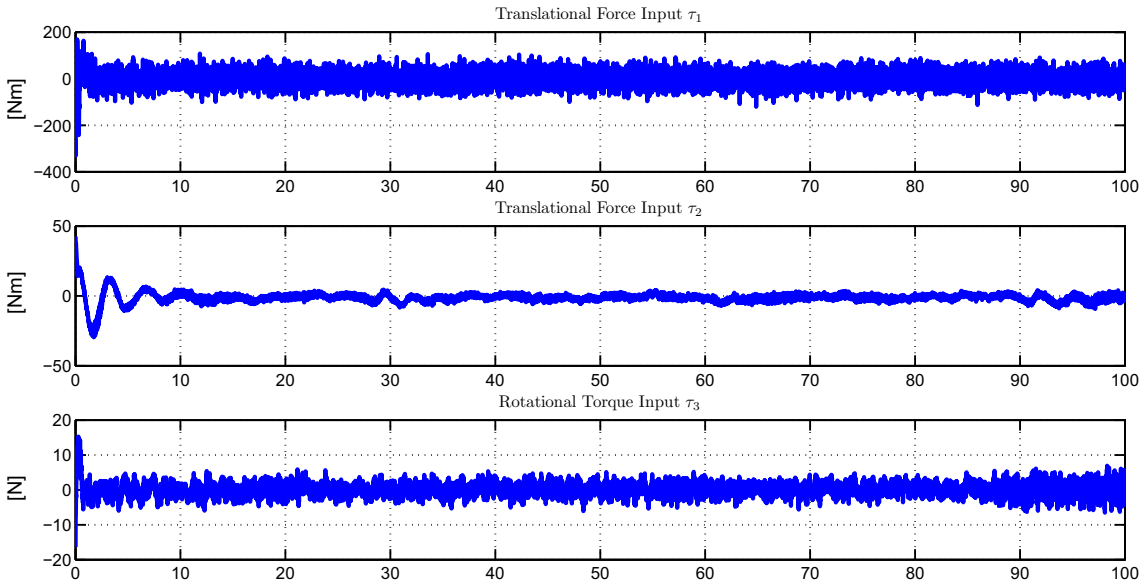

Fig. 3 Control input $\tau^*(t)$ for adaptive controller

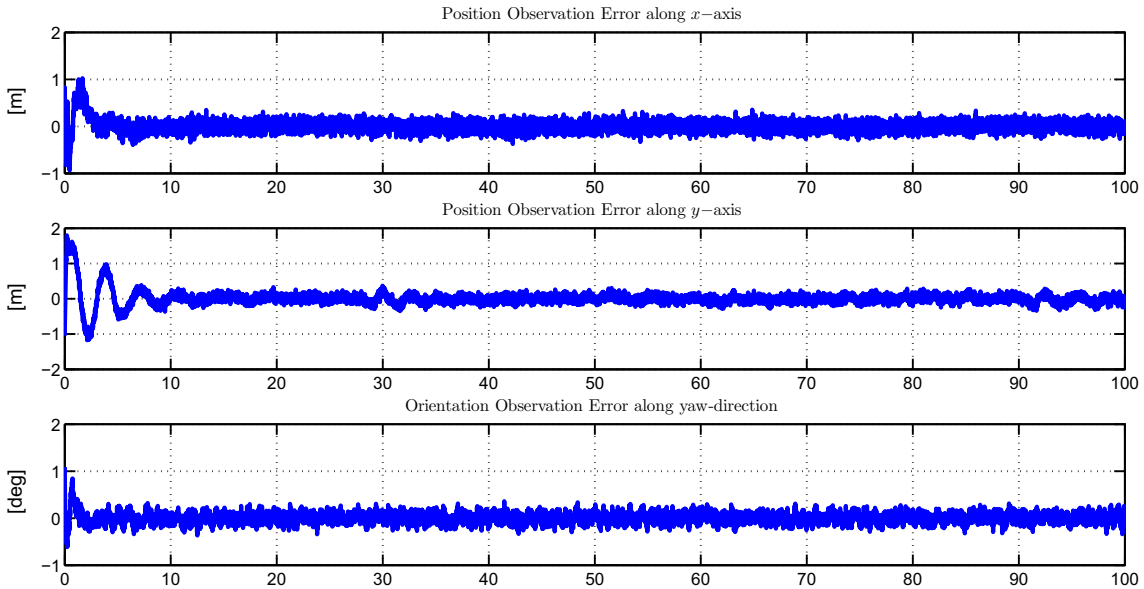

Fig. 4 Position observation error $\tilde{\eta}(t)$ for adaptive controller

$$
\begin{aligned}
K_p &= I_3, \alpha = 4.5 \\
K_0 &= diag\{\,23.93 \quad 12.14 \quad 20.007\,\} \\
K_1 &= diag\{\,0.792 \quad 0.96 \quad 0.65\,\} \\
K_c &= diag\{\,0.054 \quad 1.273 \quad 1.4\,\} \\
\Gamma &= diag\{\,0.8 \quad 1.3 \quad 0.4 \quad 1.4 \quad 0.1 \quad 0.6 \quad 0.1 \quad 0.2 \quad 1.7\,\}.
\end{aligned} \tag{77}
$$

The results are shown in Figs. 1, 2, 3, 4 and 5. In Fig. 1, the actual position $\eta(t)$ and the desired position $\eta_d(t)$ were presented. In Figs. 2 and 3, the position tracking error $e(t)$ and the control input $\tau^*(t)$ were presented, respectively. In Figs. 4 and 5 the position observation error $\tilde{\eta}(t)$ and estimation of the system parameters (*i.e.*, elements of the parameter estimate vector $\hat{\theta}(t)$) were presented, respectively. From Figs. 1 and 2, it is clear that the tracking control objective was met.

For the PID controller, controller gains were tuned via a trial-and-error method until a good tracking performance was achieved, and were chosen as

$$
\begin{aligned}
K_{p_1} &= 10, K_{i_1} = 5, K_{d_1} = 7 \\
K_{p_2} &= 14, K_{i_2} = 6, K_{d_2} = 3 \\
K_{p_3} &= 12, K_{i_3} = 8, K_{d_3} = 8
\end{aligned} \tag{78}
$$

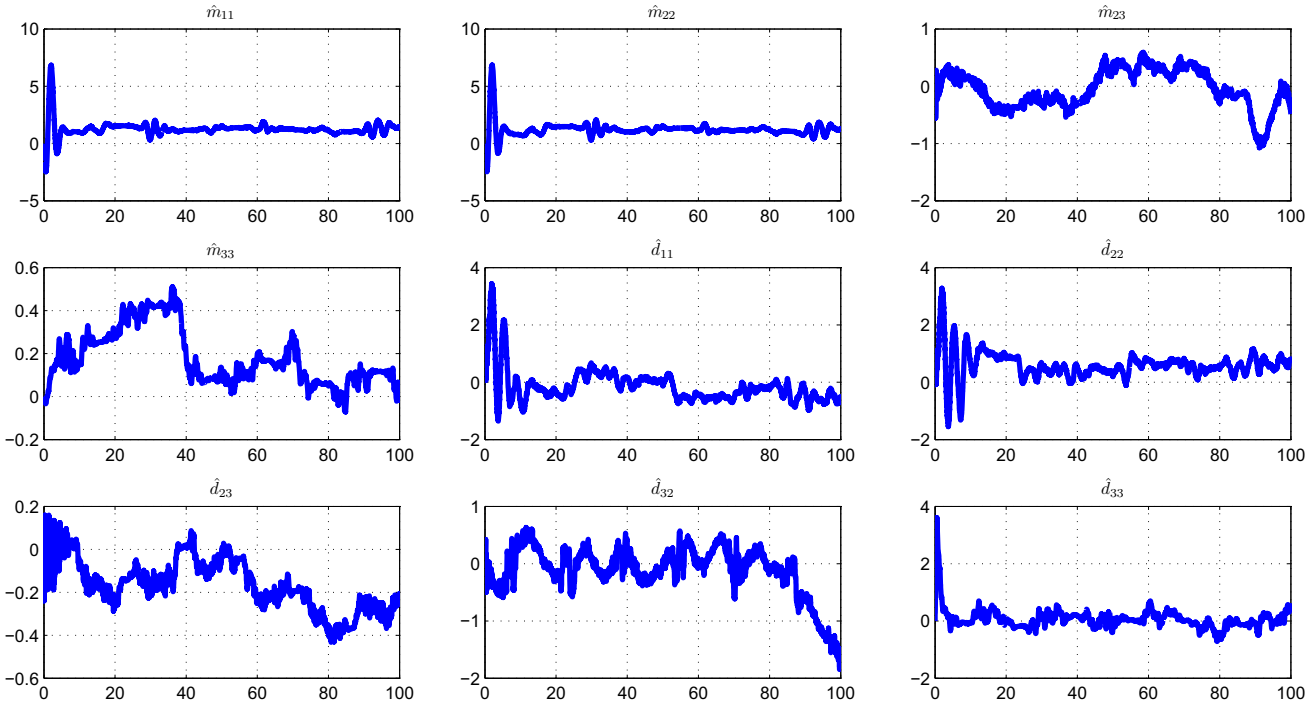

Fig. 5 Parameter estimate vector $\hat{\theta}(t)$ for adaptive controller

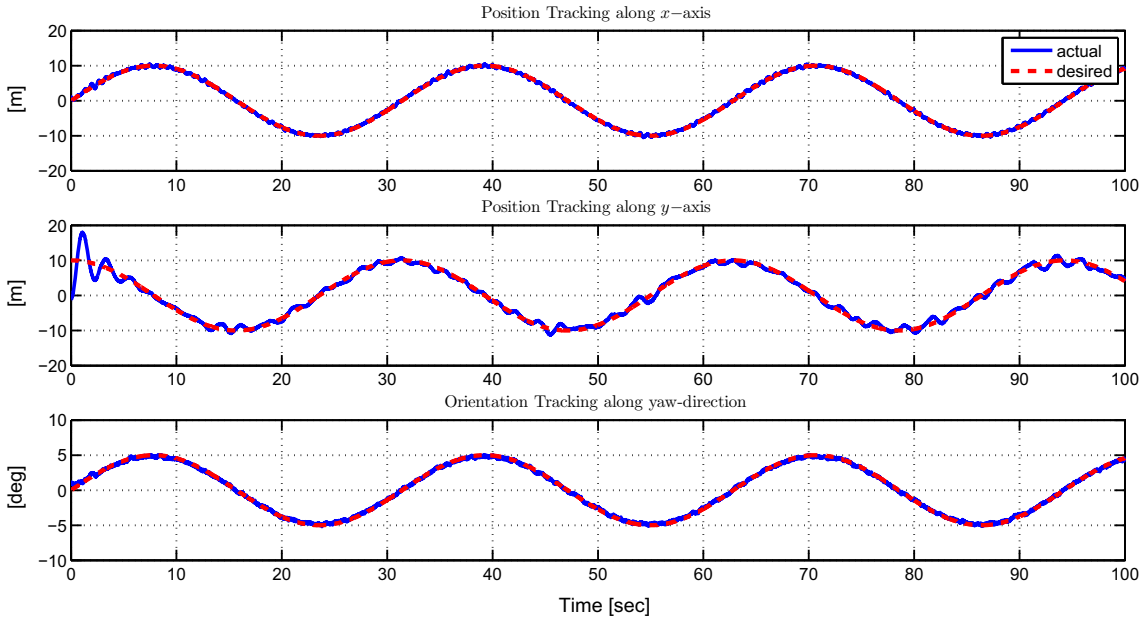

Fig. 6 The desired position $\eta_d(t)$ (*dotted*) and the actual position $\eta(t)$ (*solid*) for the PID controller

where position, integral and derivative parameters of the PID controller used for *i*th output of the system were denoted by K_{p_i}, K_{i_i} and $K_{d_i} \in \mathbb{R}$, respectively.

The results are shown in Figures 6, 7 and 8. In Fig. 6, the actual position $\eta(t)$ and the desired position $\eta_d(t)$ were presented. In Figs. 7 and 8, the position tracking error $e(t)$ and the control input $\tau^*(t)$ were presented, respectively. From Figs. 6 and 7, it is clear that the tracking control objective was met.

Square of the integral of the norm of the tracking errors (*i.e.*, $\int_{t_0}^{t} \|e(\sigma)\|^2 d\sigma$) and control inputs (*i.e.*, $\int_{t_0}^{t} \|\tau^*(\sigma)\|^2 d\sigma$) was calculated and recorded as performance measures during simulations. According to these values that are given in Table 1 numerically, it can be said that higher

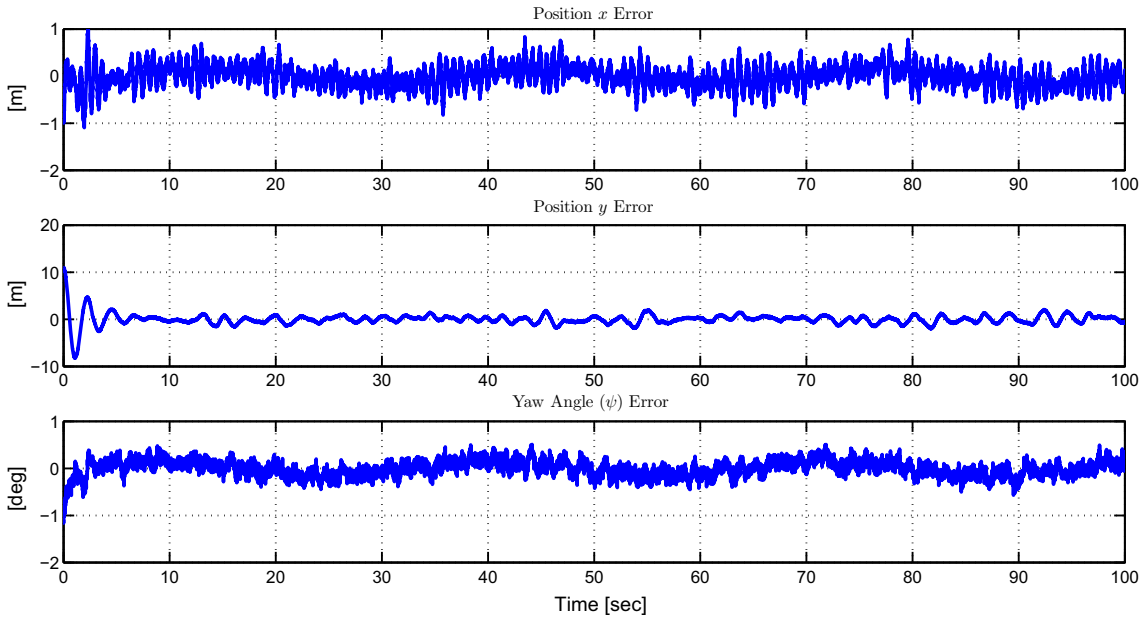

Fig. 7 The tracking error $e(t)$ for the PID controller

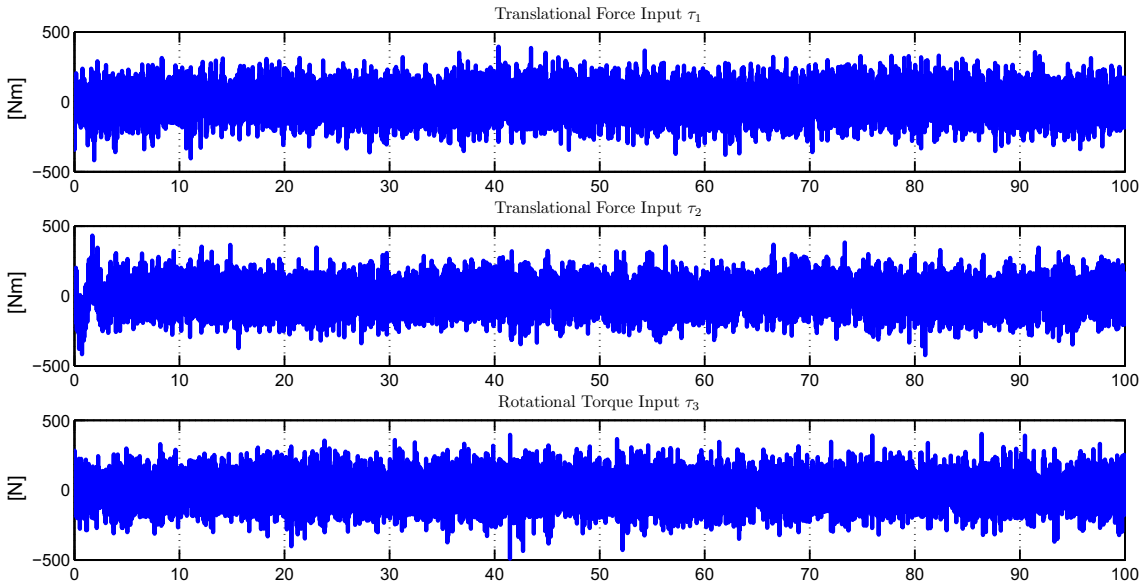

Fig. 8 Control input $\tau^*(t)$ for the PID controller

Table 1 Performance measures

Controller	$\int_{t_0}^{t} \|e(\sigma)\|^2 \mathrm{d}\sigma$	$\int_{t_0}^{t} \|\tau^*(\sigma)\|^2 \mathrm{d}\sigma$
Adaptive control	105	1.066×10^5
PID control	143	8.265×10^5

control effort was needed for PID control to obtain close tracking performance from both controllers. This difference can also be seen from the figures of the adaptive control input and figures of the PID control input given in Figs. 3 and 8, respectively.

Remark 3 As can be seen from Figs. 1, 2, 3, 4, 5, 6, 7 and 8 and performance measures presented in Table 1, the performance of the proposed controller surpasses the commercially used PID counterpart. To our best knowledge, in a simulation environment where the sensor inputs are assumed to be perfect, an output feedback controller performing better than a full state counterpart is rare. We believe this behavior is mostly due to the fast convergence of the observer formulation and the adaptive nature of the controller inserted by Eq. 29. As can be seen from (29), the adaptations insert a desired system model-based time-

varying integral effect to the system which may result in better steady state performance.

6 Conclusion

In this paper, we have presented a novel observer–controller couple backed up with a Lyapunov-type analysis. In the stability analysis, we have proven that the proposed adaptive controller design achieved semi-global tracking despite the lack of velocity measurements. Simulation results were presented to illustrate the tracking performance of the observer–controller couple.

Though this work deals with only an adaptive controller, it is our sincere belief that with considerably small effort, robust and repetitive learning versions of the same observer–controller structure can be designed to compensate for the parametric uncertainty, thus future work will focus on dealing with structured and unstructured uncertainties of the overall system.

Dynamic terms

The dynamic terms $J(\eta)$, $C(\eta,\dot{\eta})$ and $F(\eta)$ defined in (6) are calculated as follows

$$J=\begin{bmatrix} m_{11}c_\psi^2+m_{22}s_\psi^2 & (m_{11}-m_{22})s_\psi c_\psi & -m_{23}s_\psi \\ (m_{11}-m_{22})s_\psi c_\psi & m_{11}s_\psi^2+m_{22}c_\psi^2 & m_{23}c_\psi \\ -m_{23}s_\psi & m_{23}c_\psi & m_{33} \end{bmatrix}$$

$$C=\dot{\psi}\begin{bmatrix} (m_{22}-m_{11})s_\psi c_\psi & m_{11}c_\psi^2+m_{22}s_\psi^2 & 0 \\ -m_{11}s_\psi^2-m_{22}c_\psi^2 & (m_{11}-m_{22})s_\psi c_\psi & 0 \\ -m_{23}c_\psi & -m_{23}s_\psi & 0 \end{bmatrix}$$

$$F=\begin{bmatrix} d_{11}c_\psi^2+d_{22}s_\psi^2 & (d_{11}-d_{22})s_\psi c_\psi & -d_{23}s_\psi \\ (d_{11}-d_{22})s_\psi c_\psi & d_{11}s_\psi^2+d_{22}c_\psi^2 & d_{23}c_\psi \\ -d_{32}s_\psi & d_{32}c_\psi & d_{33} \end{bmatrix}.$$

Proof of bounds

In this appendix, the upper bounds of the norm of $N_b(t)$ in (40) and the norm of $\chi(t)$ in (54) will be obtained. Specifically, after utilizing (7), (8), (11), (13)–(17) along with (39), we can obtain

$$\begin{aligned}\|N_b\| \le & \frac{1}{m_l}\left\{\zeta_{j2}m_u m_l\|\ddot{\eta}_d\|+\zeta_{j2}m_l\left\|Y_d\tilde{\theta}\right\|+\zeta_{c2}\|\dot{\eta}_d\|^2+\zeta_{f2}\|\dot{\eta}_d\|+K_{p,\max}\right\}\|e\| \\ & +\frac{1}{m_l}\left\{2\zeta_{c1}\|\dot{\eta}_d\|+\zeta_{f1}+K_{c,\max}\right\}\|r\| \\ & +\frac{\zeta_{c2}\|\dot{\eta}_d\|}{m_l}\|e\|\|r\|+\frac{\zeta_{c1}}{m_l}\|r\|^2+\frac{K_{c,\max}}{m_l}\|s\|\end{aligned} \tag{79}$$

where $\|\dot{e}\| \le \|r\|$ was utilized. From the structure of (79), it is clear that the bounding constants $\rho_{0i}, i=1,\ldots,5$ can be defined as

$$\begin{aligned}\rho_{01} &\triangleq \frac{1}{m_l}\left\{\zeta_{j2}m_u m_l\|\ddot{\eta}_d\|+\zeta_{j2}m_l\left\|Y_d\tilde{\theta}\right\|+\zeta_{c2}\|\dot{\eta}_d\|^2+\zeta_{f2}\|\dot{\eta}_d\|+K_{p,\max}\right\} \\ \rho_{02} &\triangleq \frac{1}{m_l}\left\{2\zeta_{c1}\|\dot{\eta}_d\|+\zeta_{f1}+K_{c,\max}\right\} \\ \rho_{03} &\triangleq \frac{\zeta_{c2}\|\dot{\eta}_d\|}{m_l} \\ \rho_{04} &\triangleq \frac{\zeta_{c1}}{m_l} \\ \rho_{05} &\triangleq \frac{K_{c,\max}}{m_l}\end{aligned} \tag{80}$$

to obtain the upper bound of the norm of $N_b(t)$ in (40).

After substituting the definitions of $Y_d(t)\theta$ and $Y_s(t)\theta$ in (20) and (51), respectively, into the definition of $\chi(t)$ in (53), we obtain

$$\begin{aligned}\|\chi\| \le & \left\{\alpha^2 m_u+\zeta_{j1}\|\ddot{\eta}_d\|+2\alpha\zeta_{c1}\|\dot{\eta}_d\|+\zeta_{f2}\|\dot{\eta}_d\|\right. \\ & \left.+\alpha\zeta_{f1}+\zeta_{c2}\|\dot{\eta}_d\|^2+\alpha^2\zeta_{c1}\|e\|\right\}\|e\| \\ & +\left\{\alpha m_u+\zeta_{c1}\|\dot{\eta}_d\|+\alpha\zeta_{c1}\|e\|\right\}\|r\|\end{aligned} \tag{81}$$

where (7), (11), (12), (14)–(17) were utilized. When the bounding functions $\rho_1(e)$ and $\rho_2(e)$ are selected as

$$\begin{aligned}\rho_1(e) \triangleq & \alpha^2 m_u+\zeta_{j1}\|\ddot{\eta}_d\|+2\alpha\zeta_{c1}\|\dot{\eta}_d\|+\zeta_{f2}\|\dot{\eta}_d\| \\ & +\alpha\zeta_{f1}+\zeta_{c2}\|\dot{\eta}_d\|^2+\alpha^2\zeta_{c1}\|e\|\end{aligned} \tag{82}$$

$$\rho_2(e) \triangleq \alpha m_u+\zeta_{c1}\|\dot{\eta}_d\|+\alpha\zeta_{c1}\|e\| \tag{83}$$

then the bound given in (54) is obtained.

The gain condition of K_1

In this appendix, we will illustrate how the sufficient condition of (48) is obtained. After substituting the definition of $s(t)$ in (25) into (46), and then integrating $\omega(t)$ in time, we obtain

$$\begin{aligned}\int_0^t \omega(\sigma)d\sigma = & \alpha\int_0^t \tilde{\eta}^T(\sigma)(N_d(\sigma)-K_1\mathrm{Sgn}(\tilde{\eta}(\sigma)))d\sigma \\ & +\int_0^t \frac{d\tilde{\eta}^T(\sigma)}{d\sigma}N_d(\sigma)d\sigma \\ & -\int_0^t \frac{d\tilde{\eta}^T(\sigma)}{d\sigma}K_1\mathrm{Sgn}(\tilde{\eta}(\sigma))\mathrm{d}\sigma.\end{aligned} \tag{84}$$

After integrating the second integral on the right-hand side of (84) by parts, following expression can be obtained

$$\begin{aligned}\int_0^t \omega(\sigma)d\sigma &= \alpha \int_0^t \widetilde{\eta}^T(\sigma)(N_d(\sigma) - K_1 \mathrm{Sgn}(\widetilde{\eta}(\sigma)))d\sigma + \widetilde{\eta}^T(\sigma)N_d(\sigma)|_0^t \\ &\quad - \int_0^t \widetilde{\eta}^T(\sigma)\frac{dN_d(\sigma)}{d\sigma}d\sigma - \sum_{i=1}^{3} K_{1i}|\widetilde{\eta}_i(\sigma)||_0^t \\ &= \alpha \int_0^t \widetilde{\eta}^T(\sigma)\left[N_d(\sigma) - \frac{1}{\alpha}\frac{dN_d(\sigma)}{d\sigma} - K_1 \mathrm{Sgn}(\widetilde{\eta}(\sigma))\right]d\sigma \\ &\quad + \widetilde{\eta}^T(t)N_d(t) - \widetilde{\eta}^T(0)N_d(0) \\ &\quad - \sum_{i=1}^{3} K_{1i}(|\widetilde{\eta}_i(t)| - |\widetilde{\eta}_i(0)|).\end{aligned} \tag{85}$$

The right-hand side of (85) can be upper bounded as follows

$$\begin{aligned}\int_0^t \omega(\sigma)d\sigma \le \alpha \int_0^t \sum_{i=1}^{3}|\widetilde{\eta}_i(\sigma)|\left[|N_{di}(\sigma)| + \frac{1}{\alpha}\left|\frac{dN_{di}(\sigma)}{d\sigma}\right| - K_{1i}\right]d\sigma \\ + \sum_{i=1}^{3}|\widetilde{\eta}_i(t)|(|N_{di}(\sigma)| - K_{1i}) + \zeta_P.\end{aligned} \tag{86}$$

If the entries of the observer gain matrix K_1 is chosen to satisfy (48), then the following expression can be obtained

$$\int_0^t \omega(\sigma)d\sigma \le \zeta_P \tag{87}$$

and thus; from its definition in (45), it can be concluded that $P(t)$ is non-negative.

References

1. Agostinho AC, Moratelli Jr L, Tannuri EA, Morishita HM (2009) Sliding mode control applied to offshore dynamic positioning systems. Proc. of Int. Conf. on Manoeuvring and Control of Marine Craft, Guaruj (SP), Brazil, pp. 237–242
2. Balchen JG, Jenssen NA, Sællid S (1980) Dynamic positioning of floating vessels based on Kalman filtering and optimal control. In: Proc. IEEE Int. Conf. Decision and Control, Albuquerque, NM, USA
3. Balchen JG, Jenssen NA, Sællid S (1976) Dynamic positioning using Kalman filtering and optimal control theory. In: Proc. of IFAC/IFIP Symp. on Aut. in Offshore Oil Field Operation, Amsterdam, Holland, pp. 183–186
4. Bidikli B, Tatlicioglu E, Zergeroglu E (2013) Observer based output feedback tracking control of dynamically positioned surface vessels. In: Proc. of American Control Conf., Washington, DC, USA, pp. 554–559
5. Bidikli B, Tatlicioglu E, Zergeroglu E (2014) A robust tracking controller for dynamically positioned surface vessels with added mass. In: Proc. of IEEE Int. Conf. Decision and Control, Los Angeles, CA, USA, pp. 4385–4390
6. Chen M, Ge SS, How BVE, Choo YS (2013) Robust adaptive position mooring control for marine vessels. IEEE Trans Control Syst Technol 21(2):395–409
7. Fang Y, Zergeroglu E, de Queiroz MS, Dawson DM (2004) Global output feedback control of dynamically position surface vessels: an adaptive control approach. Mechatronics 14(4):341–356
8. Fjellstad O, Fossen TI (2014) Quarternion feedback regulation of underwater vehicles. In: Proc. of IEEE Int. Conf. on Control Applications, Glasgow, Scotland, pp. 857–862
9. Fossen TI, Grøvlen Å (1998) Nonlinear output feedback control of dynamically positioned ships using vectorial observer backstepping. IEEE Trans. Control Syst. Technol. 6(1):121–128
10. Fossen TI (2002) Marine control systems: guidance, navigation and control of ships, rigs and underwater vehicles. Marine Cybernetics AS, Trondheim
11. Grimble MJ, Patton RJ, Wise DA (1980) The design of dynamic positioning control systems using stochastic optimal control theory. Optimal Control Appl Methods 1(2):167–202
12. Katebi MR, Yamamoto I, Matsuura M, Grimble MJ, Hirayama H, Okamato O (2001) Robust dynamic ship positioning control system design and applications. Int J Robust Nonlinear Control 11(13):1257–1284
13. Khalil HK (2002) Nonlinear Systems, 3rd edn. Prentice Hall, New York
14. Loria A, Fossen TI, Panteley E (2000) A seperation principle for dynamic positioning of ships: theoretical and experimental results. IEEE Trans Control Syst Technol 8(2):322–343
15. Sørensen AJ, Sagatun SI, Fossen TI (1996) Design of a dynamic positioning system using model-based control. Control Eng Practice 4(3):359–368
16. Tannuri EA, Agostinho AC (2010) Higher order sliding mode control applied to dynamic positioning systems.In: Proc. of Conf. on Control Applications in Marine Systems, Rostock–Warnemnde, Germany, pp. 132–137
17. Tannuri EA, Agostinho AC, Morishita HM, Moratelli L (2010) Dynamic positioning systems: an experimental analysis of sliding mode control. Control Eng Practice 18(10):1121–1132
18. Tannuri EA, Kubota LK, Pesce CP (2006) Adaptive techniques applied to offshore dynamic positioning systems. J Braz Soc Mech Sci Eng 128(3):203–210
19. Wit CCD, Olguin E, Perrier D, Wise DA (1980) Robust nonlinear control of an underwater vehicle/manipulator system with composite dynamics. In: Proc. IEEE Int. Conf. Robot. Autom, Leuven, Belgium
20. Wondergem M, Lefeber E, Pettersen KY, Nijmeijer H (2011) Output feedback tracking of ships. IEEE Trans Control Syst Technol 19(2):442–448